Ultra-Compact Ultra-Wideband Bandpass Filter Based on Multi Mode Resonator Concept

Mostafa Danaeian, Mohammad zaboly and Meisam Yahyazadeh
[1]*Department of Electrical Engineering, Vali-e-Asr University of Rafsanjan, Rafsanjan, Iran.*
danaeian@vru.ac.ir, zabolym@gmail.com, yahyazadeh@vru.ac.ir
Corresponding Author: *danaeian@vru.ac.ir*

***Abstract*- An ultra-compact ultra-wide band (UWB) bandpass filter (BPF) with a very sharp rejection for the high-speed wireless communication applications is proposed. The functional basis of the proposed structure is based on the multi-mode resonator (MMR) technique. The suggested ultra-wideband filter is realized by using two doublet parallel coupling lines, two symmetrical open stubs and tri-section step-impedance open stubs which are located at the center of the configuration. In order to analyze the suggested configuration, the even-mode and odd-mode methods have been utilized because of the proposed UWB BPF is a symmetrical structure. Five modes which are including three even modes and two odd modes have been placed within the UWB band. By changing the dimensions of the tri-section step-impedance open stub and two symmetrical open stubs, the resonant modes of the constructed MMR can be tuned. These two parts have been mainly applied to adjust the resonant modes into desired passband. Changing the dimensions of the two symmetrical open stubs affects both the even and odd modes. But the tri-section step-impedance open stubs can only specially control the even-mode resonant frequencies, whereas the odd-mode ones are fixed. Consequently, the center frequency and the bandwidth of the proposed configuration can be simply adjusted. Experimental verification is provided and a reasonable agreement between simulated and measured results has been achieved. The proposed UWB BPF has a passband covers 3.55 to 10.65 GHz and the measured 3 dB fractional bandwidth (FBW) is about 100%. The total size of the suggested UWB BPF is about 0.76 × 0.34 λ_g^2.**

***Index Terms*-** ultra-wideband bandpass (UWB), multiple-mode resonator (MMR), step-impedance open stubs, sharp rejection and compact size.

I. INTRODUCTION

After the Federal Communications Commission (FCC) decision to permit the unlicensed operation band from 3.1 to 10.6 GHz in February 2002, the ultra-wideband (UWB) wireless communication

Manuscript received 19-July-2020 and revised 25-Sept..-2020,
Accepted on 8-Nov.-2020
P- ISSN: 2322-4088
E- ISSN: 2322-3936

technology has received great attention [1]. Decreasing cost, increasing capabilities, transmitting higher data rates and requiring lower transmit power are some of the attractive benefits of the UWB systems. However, there are a lot of challenges to meet the ultra-wide bandwidth requirement in implementing the UWB bandpass filters (BPFs). Many efforts have been carried out to realize the UWB BPFs and several types of UWB BPFs with different methods and structures have been introduced over the past few years [2-20]. Parallel-coupled microstrip lines [2], multilayer coupling structures [3], stepped impedance resonator [4-5], Ring Resonator [6-9], dual mode and multi-mode resonator (MMR) technique [10-17], are some of the several procedures and various techniques which have been proposed in the recent reported papers to implement UWB BPF. Nevertheless, these structures suffers from poor selectivity, high insertion loss, high cost, narrow upper stopband region, complexity of the manufacturing process and large size. Consequently, there is still a need to design an UWB BPF with good specifications. According to the introduced techniques, it seems that combining the multi-mode resonator (MMR) method, parallel-coupled lines procedure, stepped impedance approach and open stub loaded resonator can be a good competitive candidate for the design of the UWB BPF with high performances.

In this paper, a compact seven-pole UWB BPF with low insertion loss and sharp rejection skirts at the lower and upper edges is proposed. The proposed configuration has been implemented by using a symmetric tri-section stepped impedance resonator, two doublet parallel coupling lines and two open stubs-loaded. The basic properties of the proposed structure have been analyzed with the help of even-odd mode method. There are five modes which includes two odd modes and three even modes. These modes can be simply moved in the desired passband. Moreover, there are two transmission zeros which are located near the lower and upper edges of the passband. The proposed UWB BPF have many advantages like compact size, high selectivity, high stopband rejection, low insertion loss, and easy fabrication. Eventually, the proposed UWB BPF is designed, fabricated and tested. There is an excellent agreement between the simulated and measured results. The fractional bandwidth of the proposed UWB BPF is approximately 100%. As well as, the insertion loss is better than 1 dB and return loss is lower than 12 dB. Additionally, the variation of the group delay in the range of 3.55–10.65 GHz is less than 0.4 ns.

II. DESIGN PROCEDURE

The configuration of the proposed UWB BPF is shown in Fig.1. The introduced UWB structure is consists of two doublet parallel coupling lines, two symmetrical open stubs and the tri-section step-impedance open stubs. Five modes which are including three even modes and two odd modes have been placed within the UWB band. The parallel-coupled lines at the two sides of the suggested UWB BPF have been used to increase the coupling enhancement. The maximum amount of the coupling has

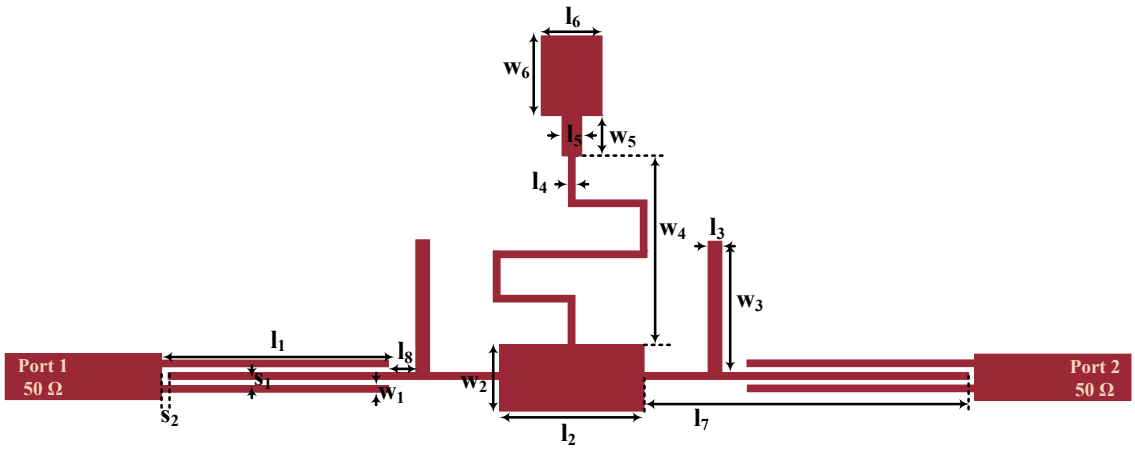

Fig.1. Configuration of the proposed UWB BPF

been adjusted near the central frequency of the UWB structure which can be varying by the length of l_1. The two symmetrical open stubs affect both the even and odd modes and are applied to regulate the last resonant mode (f_5) into the desired passband which results in sharpening the rejecting skirt of the passband in the upper edge. Additionally, two symmetrical open stubs can excite one extra transmission zero to deepen the upper stopband. The tri-section step-impedance open stubs at the central plane of the proposed UWB structure can only control the even-mode resonant frequencies, whereas the odd-mode ones are fixed. As well as, this part of the proposed structure can generate two transmission zeros near the upper and lower cutoff frequencies, leading to sharp roll-off. The schematic of the proposed MMR is illustrated in Fig. 2. Since the suggested MMR is a symmetrical structure with respect to the central dot-dashed line shown in Fig. 2 (a), the proposed MMR can be divided into two sections from the symmetry plane. Therefore, only half of the structure must be analyzed using the even-mode and odd-mode methods. The odd-mode circuit can be modeled as an electric wall added along the symmetrical plane as shown in Fig. 2 (b), whereas the even-mode circuit is achieved by adding a magnetic wall along the symmetrical plane as shown in Fig. 2 (c).

Based on Figs. 2 (b) and (c), the parallel coupling lines have an electrical length of θ_1 with characteristic admittance of Y_1. Two symmetrical open stubs have the electrical lengths of θ_2 with characteristic admittances of Y_2. The two-section step-impedance open stubs have the electrical lengths of θ_3, θ_4 with characteristic admittances of Y_3, Y_4, respectively. As well as, the next tri-section step-impedance open stubs have the electrical lengths of θ_5, θ_6, θ_7 with characteristic admittances of Y_5, Y_6, Y_7, respectively. The input admittances of the proposed MMR configuration which are shown in Fig. 2 (b) and (c), have been calculated as $Y_{in,\ even}$ and $Y_{in,\ odd}$. Accordingly, as shown in Fig. 2 (b) and (c), the transmission poles of the proposed structure can be derived.

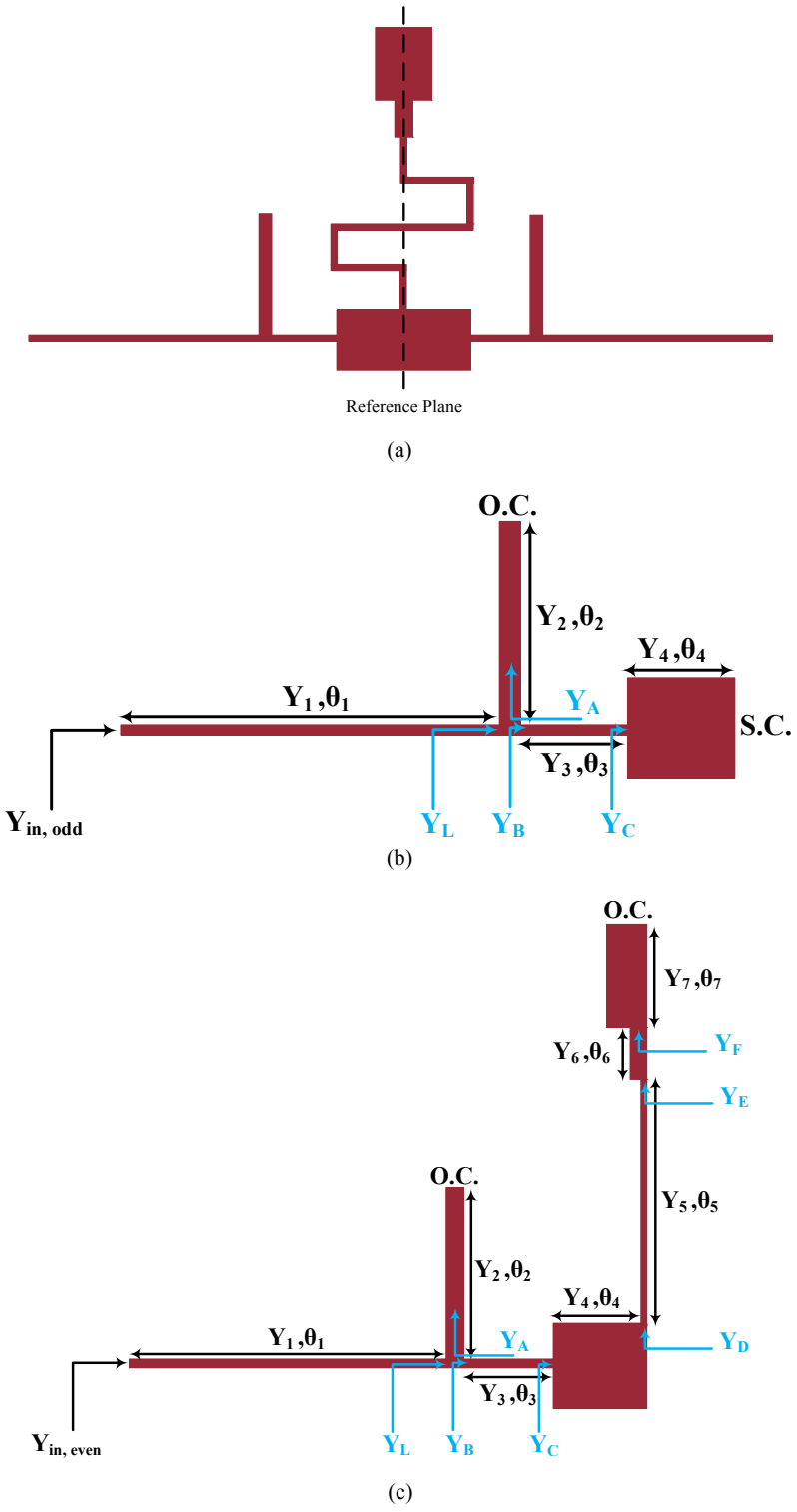

Fig.2. (a) Structure of the proposed multi-mode resonator, (b) odd-mode equivalent circuit, and (c) even-mode equivalent circuit.

Therefore, the odd mode resonance input admittance can be calculated as:

$$Y_{in,odd} = Y_1 \frac{Y_L + jY_1 \tan\theta_1}{Y_1 + jY_L \tan\theta_1} \quad (1)$$

Where

$$Y_L = Y_A + Y_B \quad (2)$$

$$Y_A = jY_2 \tan\theta_2 \quad (3)$$

$$Y_B = Y_3 \frac{jY_4 \tan\theta_4 + jY_3 \tan\theta_3}{Y_3 - Y_4 \tan\theta_3 \tan\theta_4} \quad (4)$$

$$Y_C = -jY_4 \cot\theta_4 \quad (5)$$

When $Y_{in,\,odd} = 0$, odd-mode resonance will occur.

Similarly, the even-mode input admittance can be derived as:

$$Y_{in,even} = Y_1 \frac{Y_L + jY_1 \tan\theta_1}{Y_1 + jY_L \tan\theta_1} \quad (6)$$

Where

$$Y_L = Y_A + Y_B \quad (7)$$

$$Y_A = jY_2 \tan\theta_2 \quad (8)$$

$$Y_B = Y_3 \frac{Y_C + jY_3 \tan\theta_3}{Y_3 + jY_C \tan\theta_3} \quad (9)$$

$$Y_C = Y_4 \frac{Y_D + jY_4 \tan\theta_4}{Y_4 + jY_D \tan\theta_4} \quad (10)$$

$$Y_D = Y_5 \frac{Y_E + jY_5 \tan\theta_5}{Y_5 + jY_E \tan\theta_5} \quad (11)$$

$$Y_E = Y_6 \frac{Y_F + jY_6 \tan\theta_6}{Y_6 + jY_F \tan\theta_6} \quad (12)$$

$$Y_F = jY_7 \tan\theta_7 \quad (13)$$

When $Y_{in,\,even} = 0$, even-mode resonance will occur.

Consequently, the S-parameter of the two-port network can be calculated using the following equations [2-17]:

$$S_{11} = \frac{Y_{in,even}Y_{in,odd} - Y_0^2}{\left(Y_{in,even} + Y_0\right)\left(Y_{in,odd} + Y_0\right)} \quad (14)$$

$$S_{21} = \frac{Y_{in,odd}Y_0 - Y_{in,even}Y_0}{\left(Y_{in,even} + Y_0\right)\left(Y_{in,odd} + Y_0\right)} \quad (15)$$

Where Y_0 is the characteristic impedance of the input and output ports.

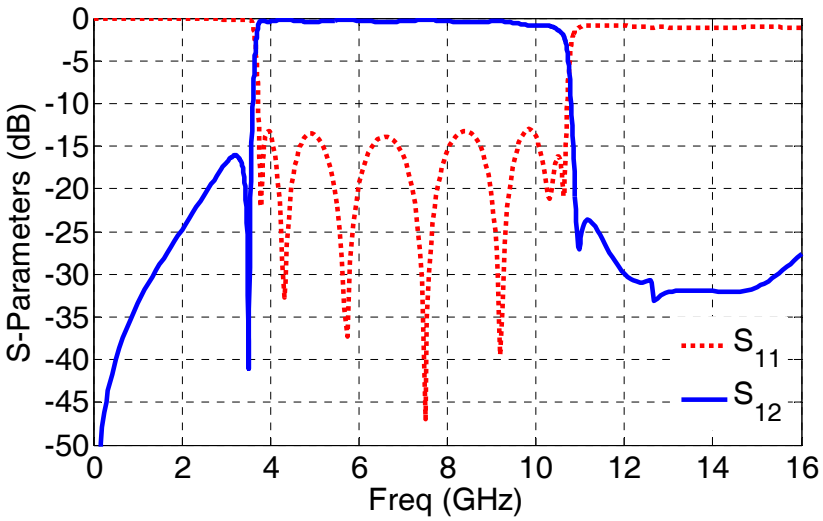

Fig. 3. Simulated frequency responses of the proposed UWB BPF.

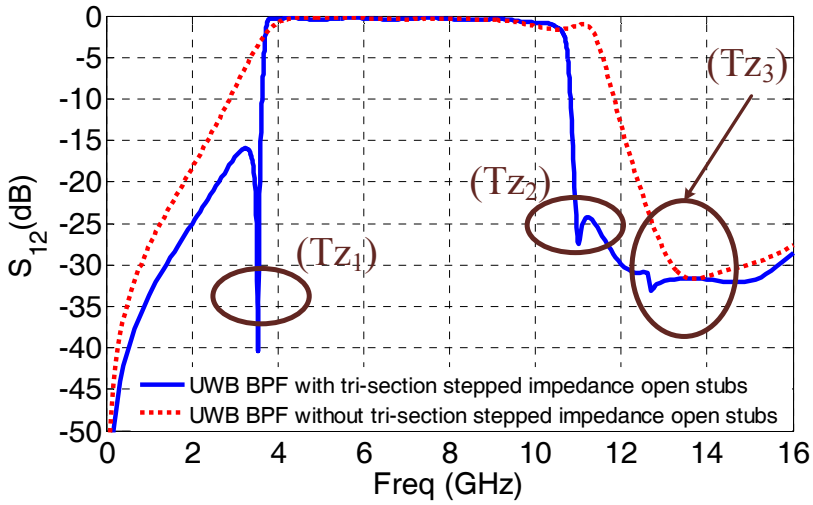

Fig. 4. Frequency responses of the proposed UWB with and without tri-section stepped impedance open stubs.

The condition of the transmission poles frequencies is achieved when $Y_{in,\,odd} = Y_{in,\,even}$ [2-17].

The simulated frequency responses of the proposed UWB BPF are presented in Fig. 3. The frequency responses of the proposed UWB BPF with and without tri-section stepped impedance open stubs are illustrated in Fig. 4. As can be seen in this figure, the frequency responses of the proposed UWB BPF without tri-section stepped impedance open stubs is not good at all. As the length l_1 of the parallel coupling lines varied from 5 mm to 7 mm which is shown in Fig. 5, the center frequency of the passband is shifted toward the lower frequency. Accordingly, the center frequency of the UWB BPF can be simply tuned by varying the length of l_1. In Fig. 6, the influence of changing the length of l_3 on the frequency response of the designed UWB BPF is depicted. As well as, the frequency responses of the proposed UWB BPF by changing the width of w_3 are illustrated in Fig. 7. According

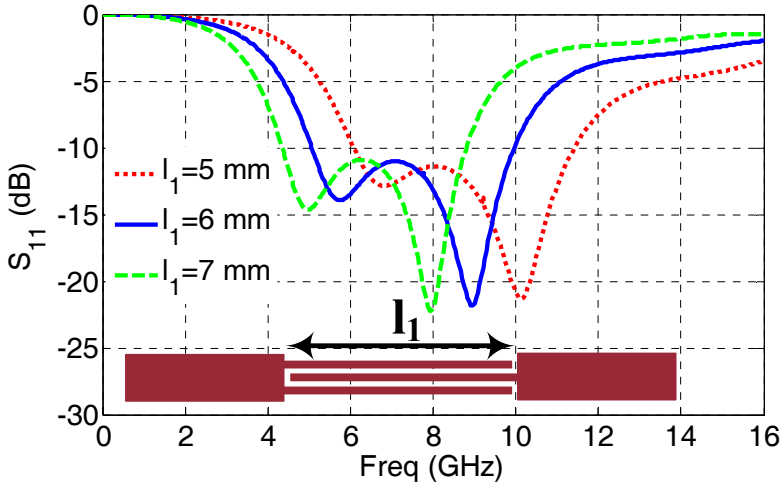

Fig. 5. Frequency response (S_{11}) of the doublets parallel coupling gaps when the length l_1 is 5 mm, 6 mm, and 7 mm, respectively.

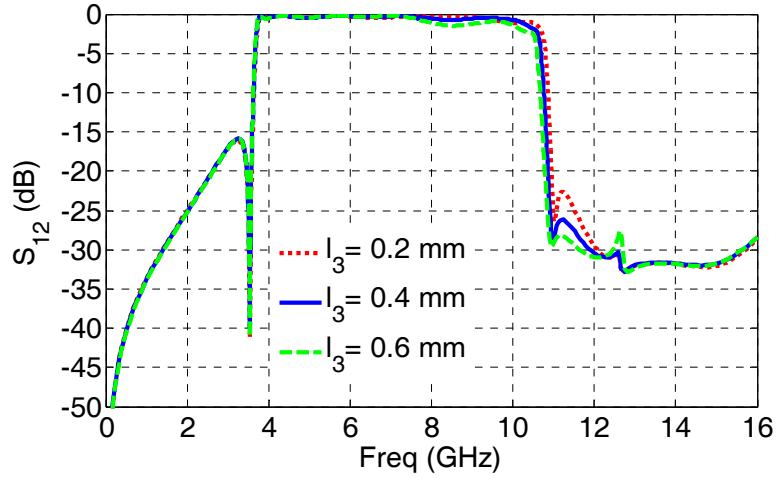

Fig. 6. Frequency responses (S_{12}) of the proposed UWB BPF when the length l_3 is 0.2 mm, 0.4 mm, and 0.6 mm, respectively.

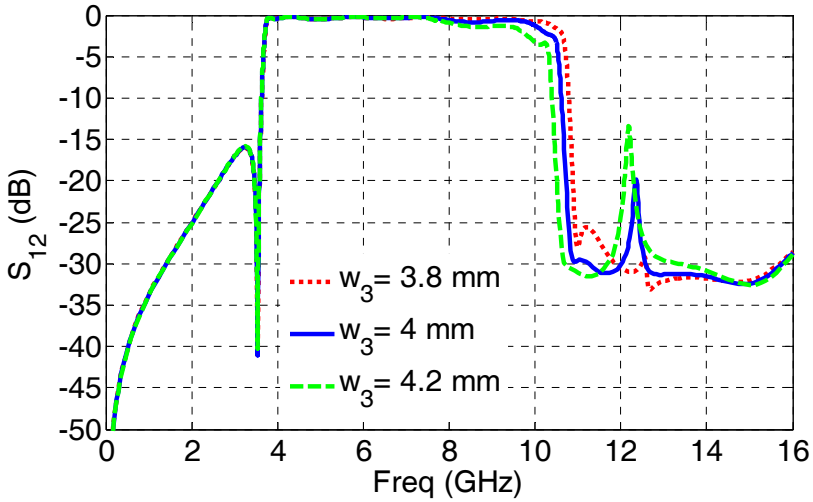

Fig. 7. Frequency responses (S_{12}) of the proposed UWB BPF when the length w_3 is 3.8 mm, 4 mm, and 4.2 mm, respectively.

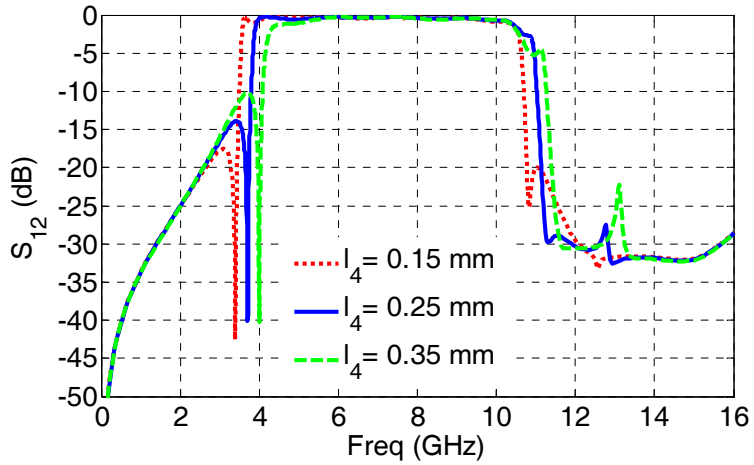

Fig. 8. Frequency responses (S_{12}) of the proposed UWB BPF when the length l_4 is 0.15 mm, 0.25 mm, and 0.35 mm, respectively.

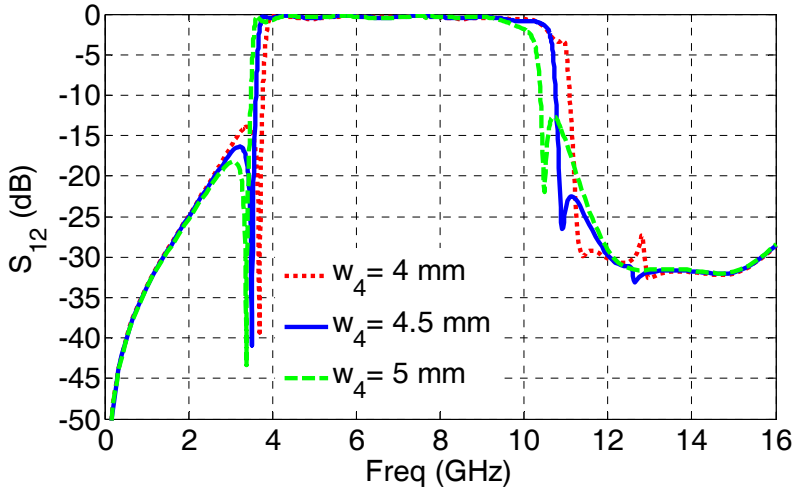

Fig. 9. Frequency responses (S_{12}) of the proposed UWB BPF when the length w_4 is 4 mm, 4.5 mm, and 5 mm, respectively.

to the Figs. 6 and 7, the bandwidth can be adjusted by changing the parameters l_3, and w_3. On the other hand, by adjusting the length and width of the tri-section step-impedance open stubs (l_4 and w_4), the five resonant modes of the proposed MMR can be regulated within the 3.1–10.6 GHz UWB band. The influence of changing the length of l_4 and width of w_4 on the frequency response of the designed UWB BPF under this condition that the other parameters unchanged are presented in Figs. 8 and 9, respectively. Fig. 10, illustrates the simulated frequency response (S_{21}) of the suggested UWB BPF with different coupling gaps in the parallel coupled lines (s_1= 0.1 mm and 0.5 mm). In this figure it can be clearly observed that there are seven transmission poles produced by the five resonant modes when the coupling of the feed lines is weak.

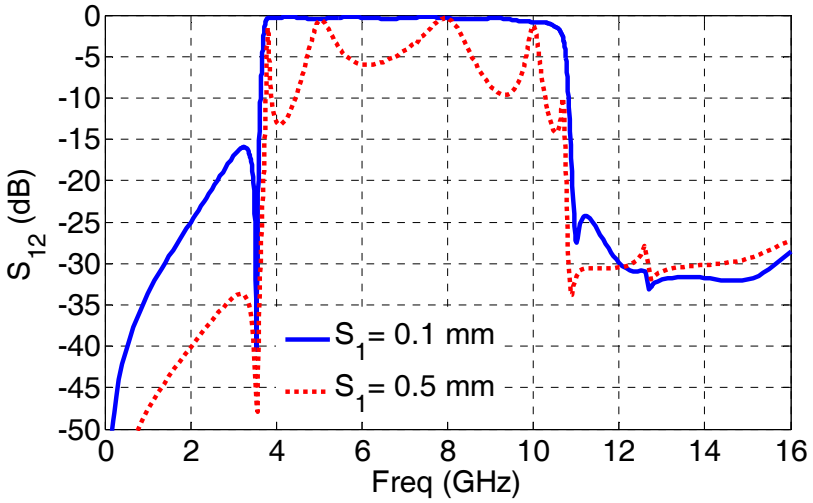

Fig. 10. Frequency responses (S_{12}) of the proposed UWB BPF with different coupling gaps

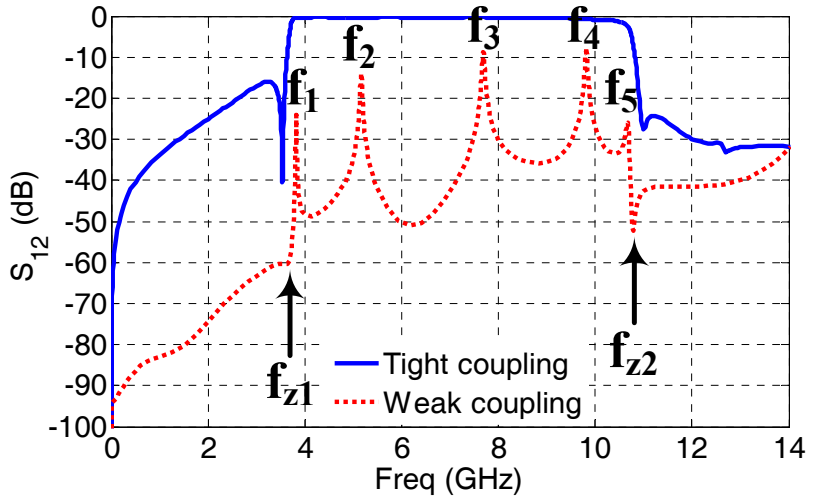

Fig.11. Simulated response (S_{12}) of the proposed UWB BPF under weak and tight coupling

As well as, the simulated frequency responses of the presented UWB BPF under weak coupling and under the tight coupling are shown in Fig. 11. Because of the symmetrical nature of the proposed UWB BPF, the theory of the even-mode and odd-mode has been used. In this Figure, f_i (i=1, 2, 3, 4, and 5) corresponds to the ith resonant frequency of the proposed MMR and f_{zj} (j=1 and 2) are the locations of the transmission zeros. From Fig. 11, it can be observed that there are five resonances in the UWB frequency band. These five modes which are including three even modes (f_1, f_3, f_5) and two odd modes (f_2, f_4), have been placed within the proposed UWB band. In the odd mode excitation, middle plane of the MMR is short-circuited. Consequently, the stepped-impedance open stub at the center could be ignored. Therefore, the parameters l_4, l_5, l_6, w_4, w_5 and w_6 do not impact on odd resonate modes, i.e. f_2 and f_4. This means that, the even mode frequencies can be adjusted by stepped-

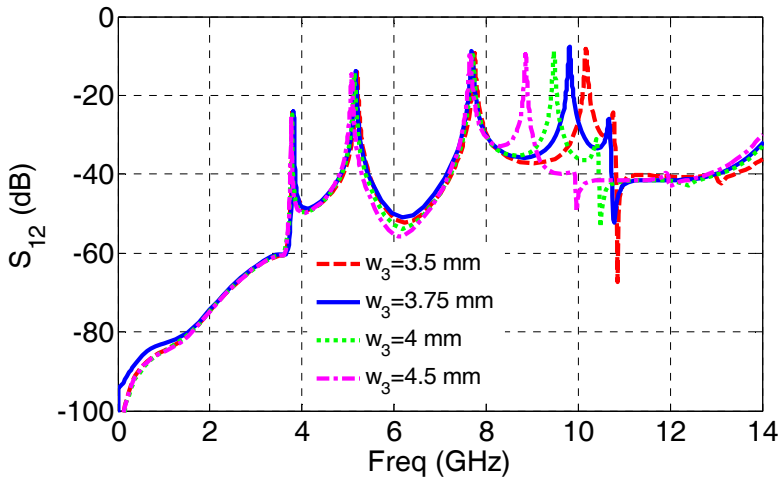

Fig.12. Resonant-mode frequencies with fixed l_3= 0.28 mm, varied w_3

impedance open stub while the odd modes are still unchanged. Thus, the even-mode resonant frequencies can be flexibly controlled by the stepped-impedance open stub at its central plane, whereas the odd-mode ones are fixed.

Moreover, two transmission zeros near the lower and upper cutoff frequencies of the passband are separately created by the tri-section step-impedance open stub leading to a high rejection skirt. Additionally, to further improve the roll-off ratio of the upper passband edges in the UWB passband, two open stubs-loaded have been added to the proposed configuration symmetrically. As can be seen in Fig. 4, when there are only two symmetrical open stubs, a transmission zero (Tz_3) is observed in the frequency response of the UWB filter (S_{12}). The location of this transmission zero is in the upper stopband which demonstrate that it helps to deepen the upper stopband. The situation of this transmission zero can be tuned by resizing the length (l_3) and width (w_3) of the two symmetrical open stubs. These transmission poles and transmission zeros are chosen to combine to form the desire UWB band. The resonant-mode frequencies of the proposed UWB BPF by changing the dimension of the width w_3 and length l_3 of the two symmetrical open stubs under the condition that the other parameters are unchanged are shown in Figs. 12 and 13, respectively. The common interpreted characteristic is that the high resonant frequencies f_4 and f_5 move towards the lower frequency, whereas the resonant frequencies f_1, f_2, and f_3 relatively remain stationary, as the l_3 and w_3 increase.

As a result of the tri-section step-impedance open stub at the symmetrical plane merely control the even modes, even-mode resonant frequencies varied the length l4 and width w4 are interpreted in Fig. 14 and Fig. 15, under the condition that the other parameters are unchanged. As the width w4 of the tri-section step-impedance open stub increased, as shown in Fig. 14, the resonant frequencies f1, f3 and f5 shift toward the lower frequency whereas the resonant frequency f2 and f3 keeps almost

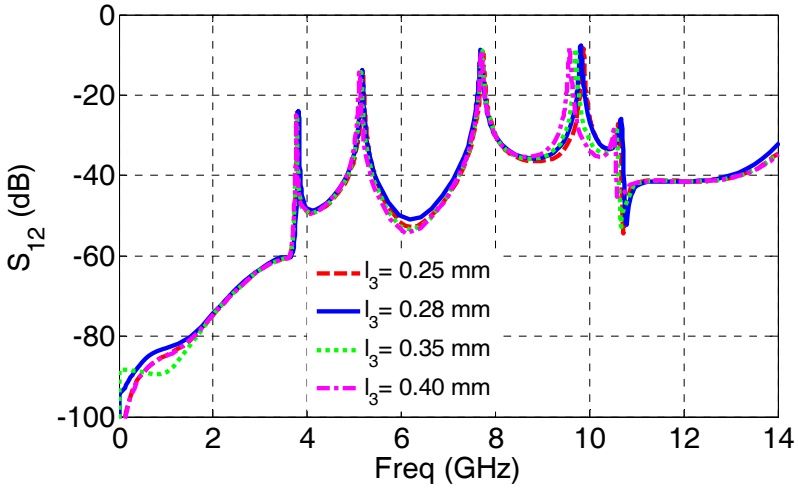

Fig.13. Resonant-mode frequencies with fixed w_3= 3.75 mm, varied l_3

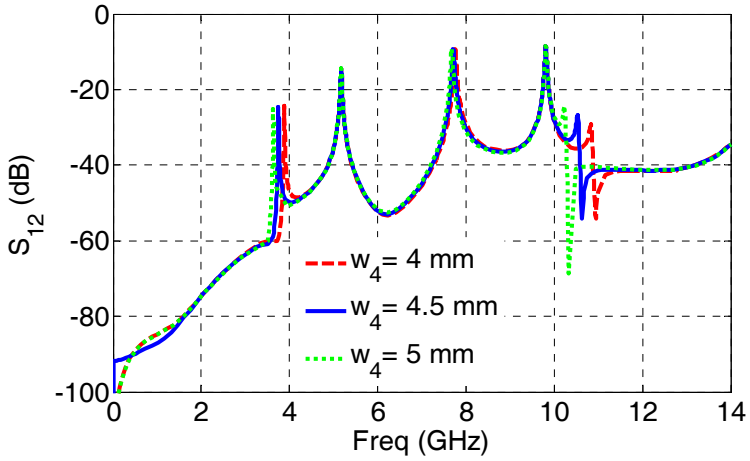

Fig.14. Resonant-mode frequencies with fixed l_4= 0.2 mm, varied w_4

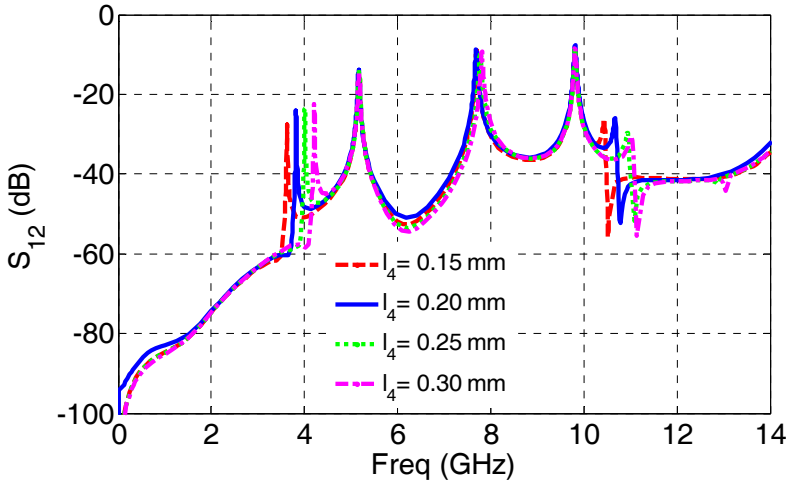

Fig.15. Resonant-mode frequencies with fixed w_4= 4.5 mm, varied l_4.

Table1: Dimensions of the proposed UWB BPF (units: mm)

l_1 = 6.15	**l_5 = 0.46**	**w_1 = 0.2**	**w_5 = 0.66**
l_2 = 5	**l_6 = 0.96**	**w_2 = 1.6**	**w_6 = 2.15**
l_3 = 0.28	**l_7 = 7.25**	**w_3 = 3.75**	**s_1= 0.1**
l_4 = 0.2	**l_8 = 0.47**	**w_4 = 4.5**	**s_2= 0.1**

unchanged. As well as, as the length l4 of the tri-section step-impedance open stub increased, as shown in Fig. 15, the resonant frequencies f1, f3 and f5 shift toward the higher frequency and the resonant frequencies f_5 shift toward the higher frequency, whereas the resonant frequency f_2 and f_3 keeps almost unchanged.

Accordingly, the design steps and optimization processes of the dimensions for the proposed UWB BPF have been summarized as follows:

1. The center frequency of the proposed UWB BPF can be adjusted by the value of l_1.

2. The bandwidth of the proposed UWB BPF can be tuned by changing the parameters l_3, l_4, w_4 and w_3.

3. The odd resonate modes of the proposed UWB BPF i.e. f_2 and f_4, can be controlled by varying the values of l_2, l_3, l_7, l_8, w_1, w_2 and w_3.

4. The even resonate mode of the proposed UWB BPF i.e. f_1, f_3 and f_5, can be regulated by varying the values of l_2, l_3, l_4, l_5, l_6, l_7, l_8, w_1, w_2, w_3, w_4, w_5 and w_6.

5. The situation of the transmission zeros can be set by resizing the parameters l_3, l_4, l_5, l_6, w_3, w_4, w_5 and w_6.

In order to facilitate the manufacturing process, all the gap widths between the strips of the parallel coupled lines in the input and output ports are chosen as 0.1 mm. The final dimensions of the proposed UWB BPF are listed in Table 1.

III. IMPLEMENTATION AND COMPARISON

A compact microstrip UWB BPF with the sharp roll-off ratio operating in the frequency range of 3.55–10.65 GHz is designed, simulated and tested. The proposed UWB BPF is implemented on a Rogers RO4003C substrate with a dielectric constant of 3.55, dielectric loss tangent of 0.0027 and a thickness of 0.8128 mm (32 mil). The frequency responses of the proposed UWB BPF have been simulated using the Advance Design System (ADS) electromagnetic simulator. In the simulations, the metallic and dielectric losses have been taken into account by using the conductivity of copper σ=5.8

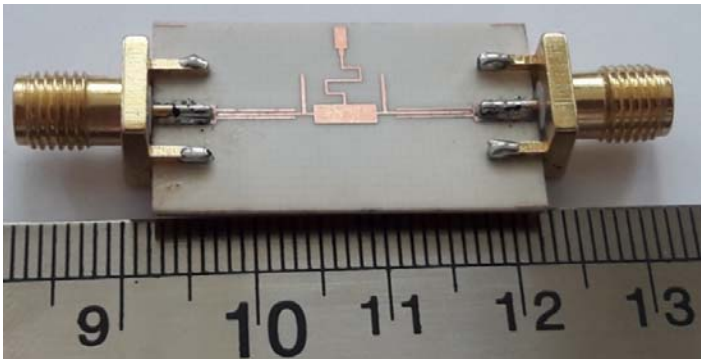

Fig. 16. Photograph of the fabricated UWB BPF.

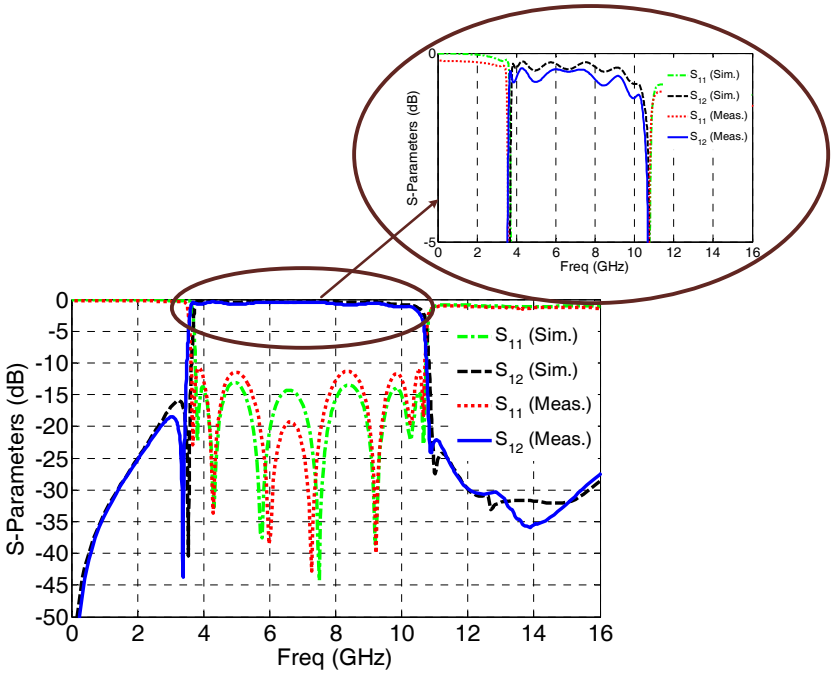

Fig.17. Simulated and measured frequency responses of the proposed UWB BPF.

× 10e^7 S/m and the loss tangent tan δ= 0.0027 for the substrate. The measured results have been achieved using a network analyzer Rohde and Schwarz, zvk. Obviously, a good agreement between the measurement and simulation results has been found. The total size of the designed UWB BPF is less than 0.77 λ_g × 0.35 λ_g (19.9 mm × 8.95 mm) where λ_g is the guided wavelength in dielectric at the central frequency. Fig. 16 depicts the photograph of a fabricated UWB BPF. The simulated and measured frequency responses of the suggested UWB BPF is presented in Fig. 17. From Fig. 17, it is shown that the measured insertion loss is less than 1 dB and the measured return loss is better than 12 dB from 3.55 to 10.65 GHz which includes the loss of two SMA connectors. In the measurement, the 3 dB UWB passband is from 3.55 to 10.65 GHz which this means that the fractional band width (FBW) is about 100%. The group delay of the proposed UWB BPF is given in Fig. 18. The group

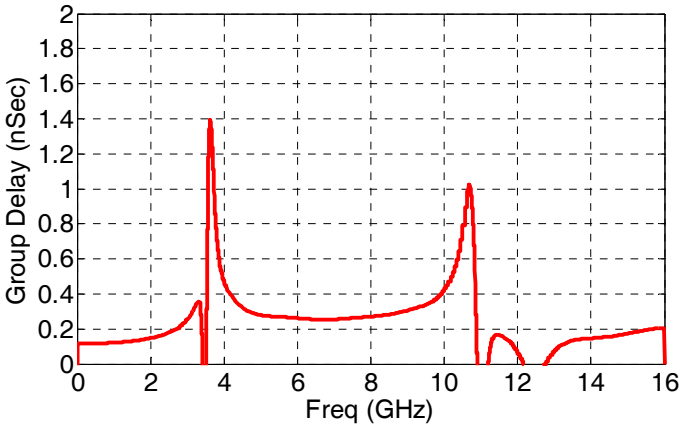

Fig. 18. Simulated group delay of the proposed UWB BPF (maximum group delay variation 0.4 ns).

delay slightly varies between 1 to 1.4 ns in the passband and the maximum variation is less than 0.4 ns over the whole UWB passband. In order to illustrate the roll-off ratio in the lower and upper passband edges, the selectivity factor (S.F.) is provided. The S.F. stands for the skirt factor of the UWB passband, defined as S.F. = $\Delta f_{3dB}/\Delta f_{30dB}$, where Δf_{3dB} and Δf_{30dB} represent for 3-dB bandwidth and 30-dB bandwidth of the passband, respectively. This parameter demonstrates that the proposed UWB BPF has high selectivity. The performance of the proposed UWB BPF compared with the other reported UWB BPFs have been summarized in Table 2. According to this table, the proposed UWB BPF has beneficial features in terms of high compactness, high selectivity, high stopband rejection, low loss, and easy fabrication.

Table 2. Comparisons of the proposed UWB BPF with the others.

Ref. number	***FBW (%)***	***IL (dB)***	***RL (dB)***	***S.F.***	***Size ($\lambda_g \times \lambda_g$)***
[5]	121	0.6	16	-	0.55×0.47
[6]	122	0.75	10.7	0.91	1.53×0.45
[7]	92	0.3	13	0.87	1.04×0.36
[11]	110	1.6	12	0.92	0.60×0.54
[13]	120	0.5	16	0.94	1.25×0.78
[15]	92	1.75	15	0.75	2.3×0.28
[17]	89	1.1	11	0.91	0.78×0.30
This Work	**100**	**1**	**12**	**0.94**	**0.76×0.34**

Abbreviations: IL: maximum in-band insertion loss; RL: return loss; S.F.: selectivity factor of the passband; Δf_{3dB}, Δf_{30dB}: 3-dB bandwidth and 30-dB bandwidth of the passband, respectively; FBW: 3-dB fractional bandwidth of passband; λ_g: the guided wavelength at center frequency.

IV. CONCLUSION

A compact UWB microstrip BPF using the multiple-mode resonator (MMR) concept is presented. Two doublet parallel coupling lines have been used to achieve much tighter coupling between the input/output port and the multiple-mode resonator. Seven poles and two zeros have been achieved by this configuration. Theoretical analysis is realized using the even-odd mode technique. The proposed resonator can generate two odd-modes and three even-modes in the desired band. The even-mode resonant frequencies can be flexibly controlled by the tri-section step-impedance open stubs, whereas the odd-mode ones are fixed. High selectivity property of the proposed UWB BPF can be adjusted by the two open stubs-loaded and tri-section step-impedance open stubs. Finally, the proposed UWB BPF has been fabricated and measured. The simulation results have been verified by the measurement results and an excellent agreement between the measured and simulated results has been achieved. Compact size, low insertion loss, high selectivity, flat group delay and good out of-band performance are the advantages of the proposed UWB BPF.

REFERENCES

[1] Federal Communications Commission, Revision of part 15 of the Commission's rules regarding ultra-wideband transmission systems, Tech. Rep., ET-Docket 98-153, FCC02-48, Apr. 2002.

[2] Siang-Wen Lan, Min-Hang Weng, Cheng-Yuan Hung, and Shoou-Jinn Chang, "Design of a compact ultra-wideband bandpass filter with an extremely broad stopband region," *IEEE Microwave and Wireless Components Letters*, vol. 26, no. 6, pp. 392-394, May 2016.

[3] Li Yang, Lei Zhu, Wai-Wa Choi, Kam-Weng Tam, Runqi Zhang, and Jianpeng Wang, "Wideband microstrip-to-microstrip vertical transition with high filtering selectivity using open-circuited slot-line SIR," *IEEE Microwave Wireless Compon Lett,* vol. 27, no. 4, pp. 329-331, March 2017.

[4] P. Kumari, M. Pal, P. Sarkar, and R. Ghatak, "UWB bandpass filter with dual-notch bands using asymmetric tri-section stepped impedance resonator," *Intern. Journal of RF and Microwave Computer-Aided Engineering*, vol. 28, no. 6, pp. e21292, Aug. 2018.

[5] Minjae Jung and Byung-Wook Min, "A highly selective UWB bandpass filter using stepped impedance stubs," *Intern. Journal of Microwave and Wireless Technologies*, vol. 10, no. 3, pp. 301-307, April 2018.

[6] T. Zhang, M. Tian, Z. Long, M. Qiao, Z. Fu, "High-temperature superconducting multimode ring resonator ultra-wide band bandpass filter," *IEEE Microwave and Wireless Components Letters*, vol. 28, no. 8, pp. 663-5, June 2018.

[7] M. Kazemi, S. Lotfi, H. Siahkamari, and M. Mohammadpanah, "UWB Bandpass Filter with Ultra-wide Stopband based on Ring Resonator," *Frequenz*, vol. 72, no. 5-6, pp. 245-252, April 2018.

[8] J. Khalilpour, "A compact and sharp ultra-wide bandpass filter by using short-stub-loaded rectangular ring and split ring resonators," *Electromagnetics*, vol. 38, no. 6, pp. 352-65, Aug. 2018.

[9] B. Wang, L. Jing, W. Huang, and F. Tan, "Ultra-Wideband Filter with Dual Notch Bands Based on Ring Resonator," *Electromagnetics*, vol. 37, no. 4, pp. 212-223, May 2017.

[10] T. Huang, Zhen Hai Shao, and Z. Chen, "Miniaturized wideband bandpass filter with enhanced selectivity and stopband suppression," *Microwave and Optical Technology Letters*, vol. 60, no. 3, pp. 769-772, March 2018.

[11] Chun-Xia Zhou, Pei-Pei Guo, K. Zhou, and W. Wu, "Design of a compact UWB filter with high selectivity and super wide stopband," *IEEE Microwave and Wireless Components Letters*, vol. 27, no. 7, pp. 636-638, June 2017.

[12] Y. Shang, W. Feng, and W. Che, "Wideband reconfigurable bandpass filter using coupled lines loaded with varactor loaded stubs," *Intern. Journal of RF and Microwave Computer-Aided Engineering*, vol. 28, no. 2, pp. e21195, Feb. 2018.

[13] L. Zhou, H. Li, Z. Long, H. Wu, T. Zhang, and M. Qiao, "Compact high temperature superconducting multi-mode ultra-wideband filter," *Microwave and Optical Technology Letters*, vol. 61, no. 2, pp. 357-360, Feb. 2019.

[14] S. Shang, B. Wei, X. Guo, B. Cao, X. Wang, L. Jiang, and X. Lu, "Superconducting wideband bandpass filter based on triple-mode resonator," *IEEE Microwave and Wireless Components Letters* vol. 28, no. 7, pp. 588-90, June 2018.

[15] L. Huang and S. Zhang, "Ultra-wideband ridged half-mode folded substrate-integrated waveguide filters," *IEEE Microwave and Wireless Components Letters*, vol. 28, no. 7, pp. 579-581, May 2018.

[16] P. Ma, B. Wei, X. Lu, Z. Xu, X. Wang, S. Shang, Bo Li, X. Guo, and B. Cao, "Synthesis Design of Wideband High-Selectivity HTS Filter by Cascading Dual-Mode Resonators," *IEEE Trans. Applied Superconductivity*, vol 28, no. 5, pp. 1-7, March 2018.

[17] M. Danaeian, E. Zarezadeh, M. H. Gholizadeh, A. R. Moznebi, and J. Khalilpour, "A Compact and Sharp Rejection Ultra-Wideband Bandpass Filter Based on Short and Open Stub-Loaded Multiple Mode Resonators," *Journal of Electrical Engineering & Technology*, vol. 15, no. 1, pp. 469-476, Jan. 2020.

[18] M. Danaeian, A. Ganji Ashkzari, K. Afrooz, and A. Hakimi, "A Compact Wide Bandpass Filter based on Substrate Integrated Waveguide (SIW) Structure," *Journal of Communication Engineering*, vol. 4, no. 2, pp. 132-141, July-Dec. 2015.

[19] S. Jamal Borhani, M. Amin Honarvar, and M. R. Namazi-Rad, "A Compact UWB Bandpass Filter with High Selectivity and Dual Notched-Band," *Journal of Communication Engineering*, vol. 4, no. 2, pp. 100-110, July-Dec. 2015.

[20] M. Hajebi, E. Zarezadeh, and F. Babaeian, "A Compact Ultra-Wideband Filter Based on Left Handed Transmission Line by Using Complementary Split Ring Resonators and Series Capacitor," *Journal of Communication Engineering*, vol. 4, no. 2, pp. 111-121, July-Dec. 2015.